OSA Proceedings on Picosecond Electronics and Optoelectronics, 1991, Vol. 9. Gerhard Sollner and Jagdeep Shah (eds.)

Femtosecond Pulses of Terahertz Radiation: Physics and Applications

D. Grischkowsky and N. Katzenellenbogen

IBM T. J. Watson Research Center, P.O. Box 218, Yorktown Heights, New York 10598

ABSTRACT

The use of high-performance, Hertzian-dipole antennas has enabled us to extend the operation of our optoelectronic, pulsed THz beam system to beyond 3 THz and to thereby, determine the limiting time-domain response function of the photoconductive switch. Via this capability, we have characterized a new type of THz source producing 380 fsec pulses, the shortest directly measured THz pulses in free space to date.

A high-brightness pulsed THz beam system has been recently developed (1). This optoelectronic system is based on repetitive, fsec optical excitation of a Hertzian dipole antenna (1,2) embedded in a charged coplanar transmission line structure. The resulting synchronous bursts of radiation are collimated by a THz optical system into a diffraction-limited beam and focused onto a similar receiver. The THz system has quite tight coupling between the transmitter and receiver, while the good focusing properties preserve the ultrafast time dependence of the source. Transmitted waveforms have been measured with subpsec resolution and with signal-to-noise ratios of more than 10,000:1.

In this paper we extend the work of Ref. (1) to smaller antennas and thereby, increase the frequency response to 3 THz. From the calculated THz optical transfer function together with the known THz absorption, we extract the limiting bandwidth of the system. Because the transmitter and receiver are identical, identical transmitter and receiver bandwidths are obtained. This result is compared to the calculated radiation spectrum from a Hertzian dipole (2,3) driven by the current pulse determined by the laser pulsewidth, the current risetime, and the carrier lifetime. From this comparison, the time-domain response function for the antenna current is obtained. We then use the receiver response function to extract the true bandwidth of a novel source of relatively powerful and extremely short pulses of freely propagating THz radiation (4). These pulses, having a measured (full-width-at-half-maximum) pulsewidth of 380 fsec with no deconvolution, are the shortest directly-measured, freely-propagating THz pulses in free space to date.

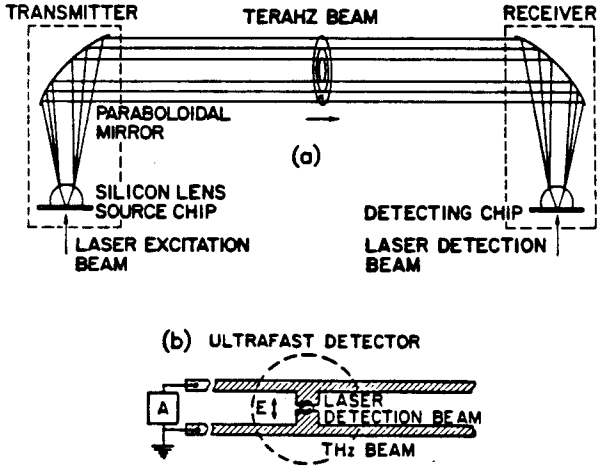

Fig.1 (a) THz optics, (b) Receiving antenna.

The optoelectronic THz beam system (1) is shown in Fig. 1a. In general, laser excitation of the source chip produces a burst of THz radiation. A large fraction of the radiation is emitted into the substrate in a cone normal to the interface and is then collected and collimated by a high-resistivity (10 kΩcm) crystalline silicon lens attached to the back side of the chip (5). A colliding-pulse, mode-locked (CPM) dye laser provides the 623 nm, 60 fsec excitation pulses at a 100 MHz repetition rate in a beam with an average power of 7 mW on the excitation spot. After collimation by the lens, the beam of THz pulses propagates and diffracts to a paraboloidal mirror, where the THz radiation is recollimated into a highly directional beam. After further propagating 50 cm the THz beam is incident upon the receiver, where a second matched paraboloidal mirror focuses the beam onto a second identical silicon lens, which in turn focuses it onto an ion-implanted SOS detection chip with the antenna geometry shown in Fig. 1b. The antenna structure is located in the middle of a 20-mm-long coplanar transmission line consisting of two parallel 5-μm-wide aluminum lines separated from each other by 10 μm. The electric field of the focused incoming THz radiation induces a transient bias voltage across the 5 μm gap between the two arms of this receiving antenna, directly connected to a low-noise current amplifier. The amplitude and time dependence of this transient voltage is obtained by measuring the collected charge (average current) versus the time delay between the THz pulses and the delayed CPM laser pulses in the 5 mW detection beam. These pulses synchronously gate the receiver, by driving the photoconductive switch defined by the 5 μm antenna gap.

For the transmitting antenna shown in Fig. 2a, identical to the receiving antenna and also fabricated on ion-implanted SOS, we measure the transmitted THz pulse shown in Fig. 2b. This pulse is shown on an expanded time scale in Fig. 2c, where the measured FWHM pulsewidth of 420 fsec (with no deconvolution) is indicated. This pulsewidth is significantly shorter than the 540 fsec pulse obtained from the same experimental arrangement, but with 30-μm-long antennas (1). The use of antennas smaller than Fig. 2a did not significantly shorten the THz pulses. The numerical Fourier transform of Fig. 2b is shown in Fig. 2d, where the amplitude spectrum is seen to extend beyond 3 THz. The sharp spectral features are water lines (6), from the residual water vapor present in the apparatus.

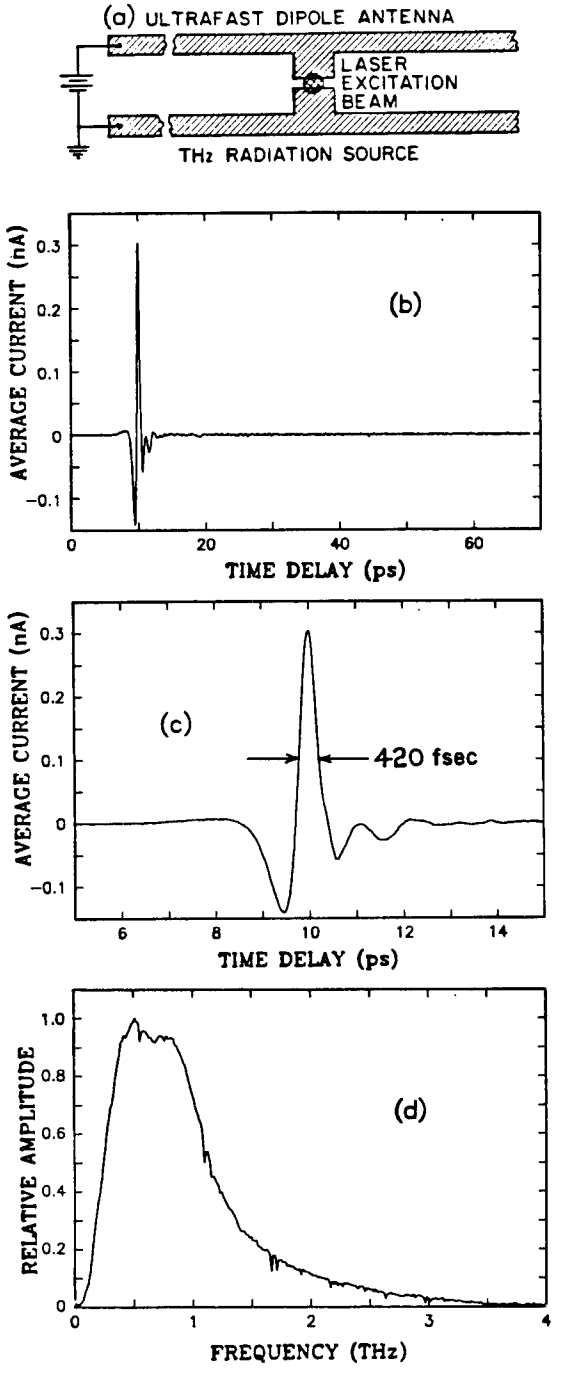

Fig.2 (a) Transmitting antenna, (b) Measured THz pulse, (c) Measured THz pulse on expanded time scale, (d) Amplitude spectrum of Fig. 2b.

Two effects reduce the spectral extent of the measured pulse (Fig. 2d). These are the frequency-dependent transfer function (7) of the THz optical system (Fig. 1a) and the THz absorption in the sapphire (SOS) chips (5). The transmission function describing these two effects is presented in Fig. 3a. Dividing the measured spectrum in Fig. 2d by this transmission function we obtain Fig. 3b. Here, the spectral extent is determined only by the product of the receiver response and the transmitted spectrum. Because the transmitter and receiver are identical, by the reciprocity theorem (8), the transmitted spectrum is identical to the receiver response, and is given by the square root of Fig.3b shown in Fig. 3c.

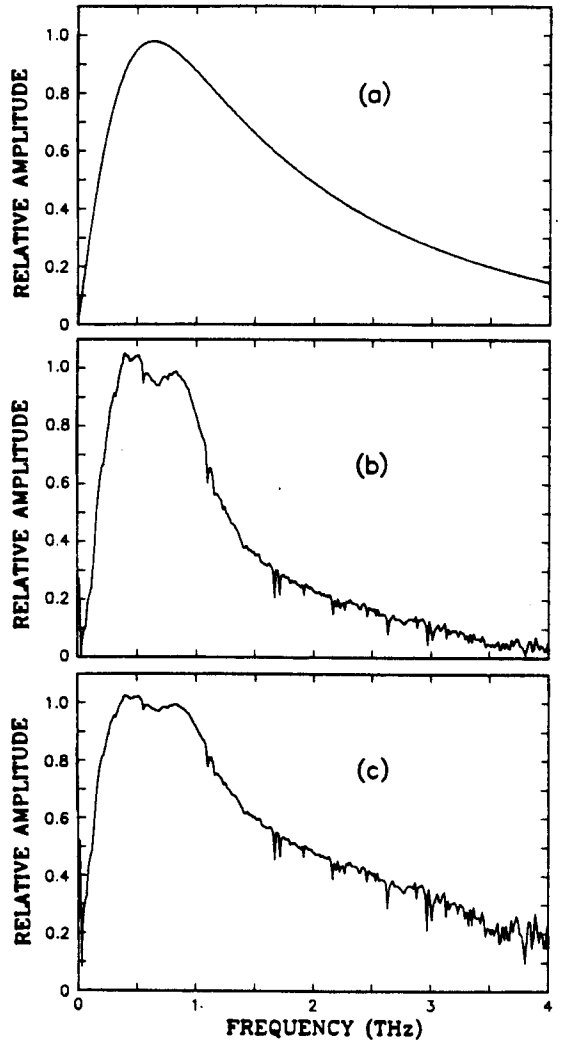

Fig.3 (a) Transmission function, (b) Amplitude spectrum of Fig. 2c divided by transmission function, (c) Amplitude spectral response of transmitter and receiver.

In the small antenna limit corresponding to the Hertzian dipole (2,3), the generated radiation field is proportional to the time-derivative of the current pulse. Based on our results we conclude that the current in the antenna is mainly determined by the intrinsic response of the semiconductor itself. We will now briefly derive the intrinsic time-domain response function for a semiconductor described by the simple Drude formalism. For this case the free carriers are considered as classical point charges subject to random collisions. Here we use the simplest version of this model for which the collision damping is independent of the carrier energy and for which the frequency dependent complex conductivity $\sigma(\omega)$ is given by (9)

$$\sigma(\omega) = \sigma_{dc} \frac{i\Gamma}{\omega + i\Gamma}, \tag{1}$$

where $\Gamma=1/\tau$ is the damping rate and τ is the average collision time. This relationship is in good agreement with recent time-domain spectroscopy measurements on lightly doped silicon from low frequencies to beyond 2 THz (9). The dc conductivity is given by $\sigma_{dc} = e\mu_{dc}N$, where e is the electron charge, μ_{dc} is the dc mobility and N is the carrier density. In the following discussion it is helpful to cast the formalism into a frequency dependent mobility as

$$\mu(\omega) = \mu_{dc} \frac{i\Gamma}{\omega + i\Gamma}, \tag{2}$$

The dc current density is given by $J_{dc} = \sigma_{dc}E$, or equivalently $J_{dc} = eE\mu_{dc}N$, where E is a constant electric field. Because of the linearity of the current in N, for a time dependent carrier density N(t), the time dependent current density can be written as

$$J(t) = eE\int_{-\infty}^{t} \mu(t - t')N(t')dt', \tag{3}$$

where μ(t-t') is the time-domain response function for the mobility. This function is determined by the inverse transform of the frequency dependent mobility to be the causal function

$$\mu(t - t') = \mu_{dc}\Gamma e^{-\Gamma(t - t')} \tag{4}$$

which vanishes for negative (t-t').

In order to facilitate the understanding of the photoconductive switch it is useful to rewrite the basic Eq. (3) in the equivalent form,

$$J(t) = eEA\int_{-\infty}^{t} \mu(t-t')\int_{-\infty}^{t'} R_c(t'-t'')I(t'')dt''dt', \tag{5}$$

where I(t'') is the normalized intensity envelope function of the laser pulse, A is a constant giving the conversion to absorbed photons/volume and R_c describes the decay of the photogenerated carriers. By defining a new photocurrent response function j_{pc}(t-t'), we can rewrite Eq.(5) in the following form

$$J(t) = \int_{-\infty}^{t} j_{pc}(t-t')I(t')dt', \tag{6}$$

where j_{pc}(t-t') is obtained by evaluating Eq.(5) with a delta function δ(t'') laser pulse. Assuming the causal function R_c(t'-t'')= exp-(t'-t'')/τ_c, describing a simple exponential decay of the carriers with the carrier lifetime τ_c (significantly longer than the average collision time τ) for positive (t'-t'') and vanishing for negative (t'-t''), and that μ(t-t') is given by the Drude response of Eq. (4), the causal response function j_{pc}(t*) is then evaluated to be

$$j_{pc}(t^*) = \frac{\mu_{dc}eEA\Gamma}{\Gamma - 1/\tau_c}\left(e^{-t^*/\tau_c} - e^{-t^*/\tau}\right) \tag{7}$$

for positive t*= (t-t') and shown to vanish for negative t*. In the short pulse limit of the ultrafast excitation pulses, the time dependence of the photocurrent J(t) is approximately equal to that of the photocurrent response function j_{pc}(t*) for positive t*. For a long carrier lifetime, the time dependence of j_{pc}(t*) is described by a simple exponential rise with a risetime of the order of τ=1/Γ, which is equal to 270 fsec and 150 fsec for the electrons and holes, respectively, in lightly doped silicon (9). As these results show, the material response can be slow compared to the duration of the ultrafast laser excitation pulses which can be as short as 10 fsec, but is more typically of the order of 60 fsec.

For the photoconductive switches considered here, we assume the time-domain response function j_{pc}(t*) to have the time dependence described by Eq. (7). This response function is

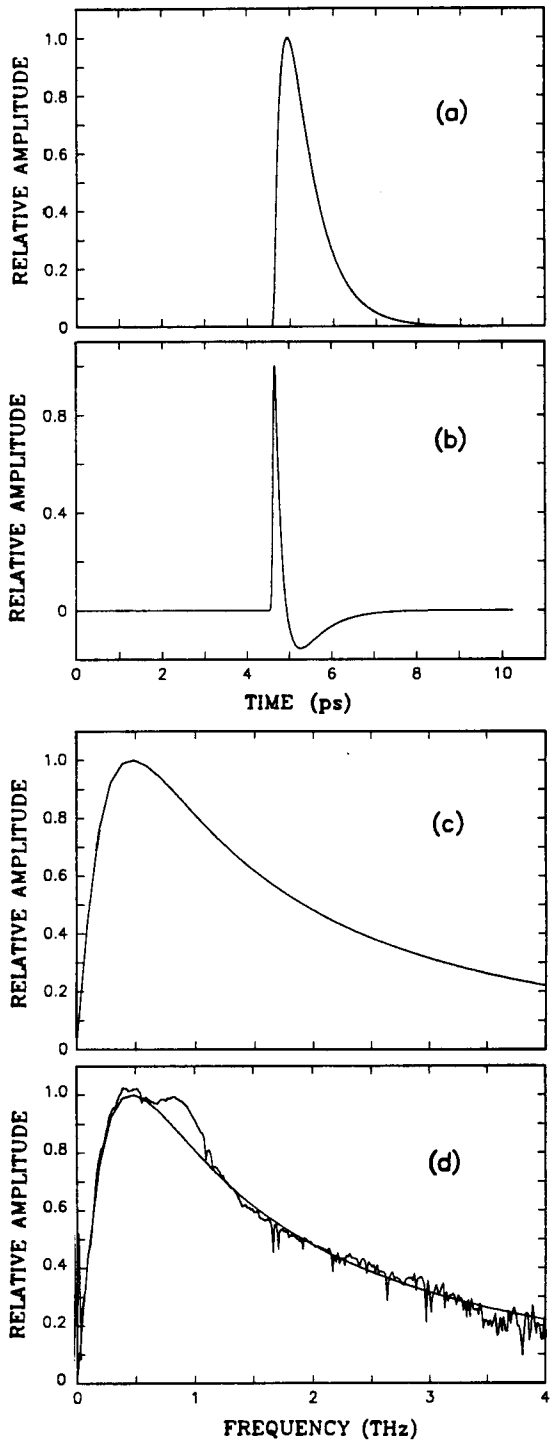

Fig.4 (a) Calculated current pulse in antenna, (b) Time-derivative of current pulse, (c) Amplitude spectrum of Fig. 4b, (d) Comparison of Figs. 4c and 3c.

then correlated with a Gaussian shaped laser pulse with a FWHM of 60 fsec. The carrier lifetime τ_c has been measured to be 600 fsec for ion-implanted SOS (10). As demonstrated above good agreement with experiment is obtained with the average collision time τ = 190 fsec. With these parameters the calculated shape of the current pulse in the photoconductive switch and the Hertzian dipole antenna is presented in Fig. 4a. The time derivative of this pulse is given in Fig. 4b, where an extremely fast transient, corresponding to the rising edge of the current pulse, is seen. The numerical Fourier transform of Fig. 4b, presented in Fig. 4c, is the predicted amplitude spectrum of the transmitter. In Fig. 4d, this spectrum is compared with the amplitude spectrum of the transmitter from Fig. 3c; the agreement is excellent. Thus, we have determined an experimentally self-consistent time-domain response function describing the current in the dipole antenna, although the 190 fsec risetime (collision time) seems too slow for ion-implanted SOS.

The well-characterized THz beam system and ultrafast detector of Fig. 1 can now be used to determine the spectral response of a new source of extremely short pulses of THz radiation (4). The operatic ı of this source is based on a recently discovered optoelectronic effect (11), initially used to generate 350 fsec electrical pulses on a coplanar transmission line by focusing ultrafast laser pulses on the interface (edge) of the positively biased line. Here, as illustrated in Fig. 5a, we use the same technique with a different line geometry and together with the THz beam system to capture the radiation emitted into the substrate from the point of excitation. The 20-mm long coplanar transmission line structure consists of two 10-μm-wide, Ni-Ge-Au metal lines separated by 80 μm and fabricated on intrinsic, high-resistivity GaAs. Irradiating the edge of the positively biased line with focused 10 μm-diameter, ultrafast laser pulses produces synchronous bursts of electromagnetic radiation. This source is completely compatible with the THz beam system and merely replaces the source chip.

The measured THz pulse emitted from the laser excited metal-GaAs interface with +60V bias across the transmission line is shown in Fig. 5b, and on an expanded time scale in Fig. 5c. The feature (dip) on the falling edge of the THz pulse

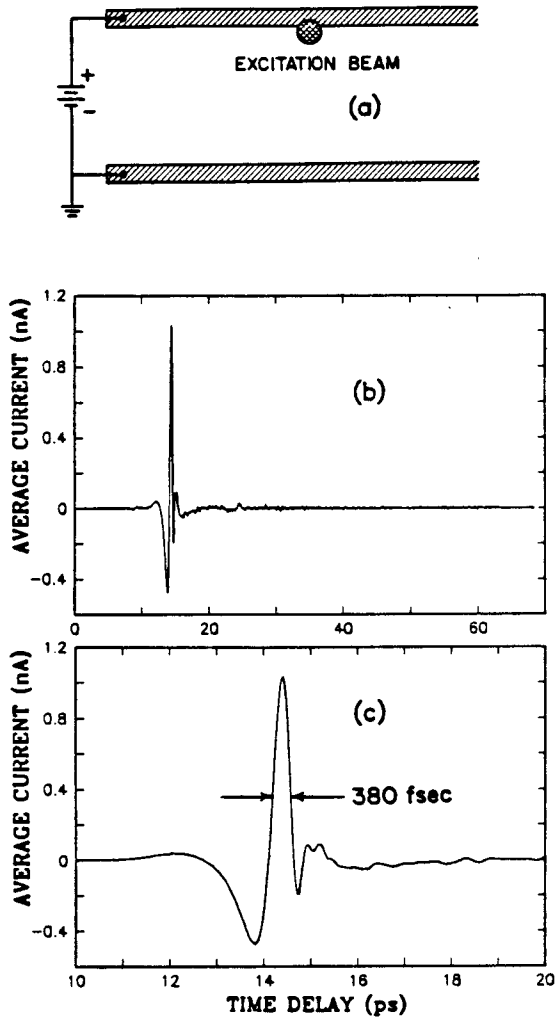

Fig.5 (a) New method to generate pulses of THz radiation, (b) Measured THz pulse, (c) Measured THz pulse on an expanded time scale.

is the sharpest feature ever measured with an ion-implanted, SOS detector. The dip is caused by the pulse reshaping due to the dispersive (5) propagation of the ultrashort THz pulse through the 0.46-mm-thick GaAs generation chip and the 0.46-mm-thick sapphire substrate of the SOS detection chip. Because of the exceptionally low dispersion and absorption of silicon (5), the 13.5 mm propagation through the silicon lenses does not significantly effect the pulseshape. The measured 190 fsec time delay from the minimum of the dip to the next later maximum, demonstrates an exceptionally fast receiver

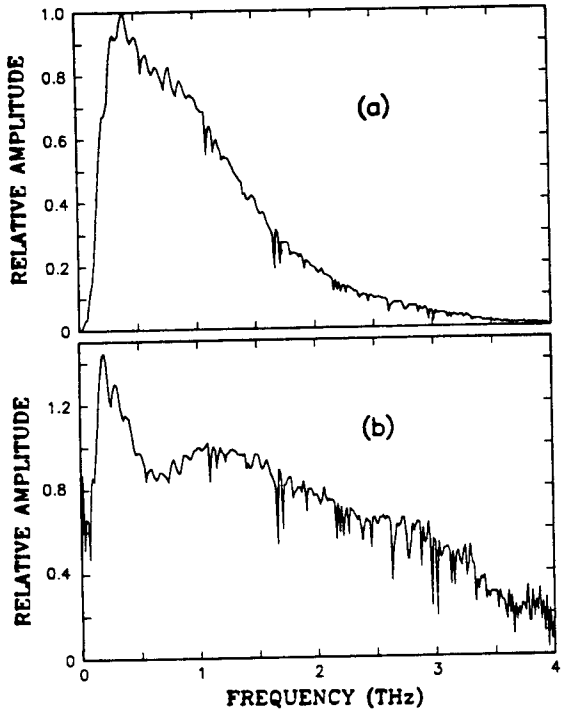

Fig.6 (a) Amplitude spectrum of Fig.5b, (b) Amplitude spectrum (Fig. 6a) divided by the transmission function (Fig.3a) and by the receiver response (Fig. 4c).

response time, consistent with the time-domain response function describing the current in the receiving antenna as given by Eq. (7).

The numerical Fourier transform of the pulse of Fig. 5b, as presented in Fig. 6a, is only a lower limit to the true spectral extent. However, by using the above information characterizing the THz beam system, we can now access the true spectral response of this source. Accordingly, the spectrum in Fig. 6a is divided by the transmission function (Fig. 3a) and then divided by the receiver frequency response (Fig. 4c). The result shown in Fig. 6b illustrates the broad spectrum of this source. Again, the sharp line structure is due to water absorption lines (6).

ACKNOWLEDGMENTS

We acknowledge stimulating and informative conversations with Stephen Ralph and Joshua Rothenberg. Martin van Exter initially calculated the THz optical transfer function and an early version of the time-domain response function. Søren Keiding made some preliminary measurements on the GaAs based source. The excellent masks and wafer fabrications were done by Hoi Chan.

REFERENCES

1. Ch. Fattinger and D. Grischkowsky, Appl. Phys. Lett., Vol. 53, 1480 (1988); Vol. 54, 490 (1989); Proc. Picosecond Electronics and Optoelectronics Topical Meeting (Salt Lake City, UT), Mar. 8-10, 1989, p225; M. van Exter, Ch. Fattinger, and D. Grischkowsky, Appl. Phys. Lett., Vol. 55, 337 (1989); M. van Exter and D. Grischkowsky, IEEE Trans. Microwave Theory Tech., Vol.38, 1684 (1990).
2. P.R. Smith, D.H. Auston, and M.C. Nuss, IEEE J. Quantum Elect. Vol. 24, 255 (1988).
3. D.H. Auston, K.P. Cheung, and P.R. Smith, Appl. Phys. Lett., Vol. 45, 284 (1984).
4. N. Katzenellenbogen and D. Grischkowsky, Appl. Phys. Lett., Vol. 58, 222 (1991).
5. D. Grischkowsky, S. Keiding, M. van Exter and Ch. Fattinger, J. Opt. Soc. Am. B, Vol.7, 2006 (1990).
6. M. van Exter, Ch. Fattinger, and D. Grischkowsky, Optics Lett., Vol.14, 1128, (1989).
7. J.C.G. Lesurf, "Millimetre-Wave Optics, Devices & Systems", (Adam Hilger, Bristol, England, 1990).
8. G.D. Monteath, "Applications of the Electromagnetic Reciprocity Principle", (Pergamon Press, Oxford, 1973).
9. Martin van Exter and D. Grischkowsky, Phys. Rev. B., Vol. 41, 12 140 (1990)
10. F.E. Doany, D. Grischkowsky, and C.-C. Chi, Appl. Phys. Lett., Vol. 50, 460 (1987).
11. D. Krökel, D. Grischkowsky, and M.B. Ketchen, Appl. Phys. Lett., Vol. 54, 1046 (1989).